Cancer Letters 442 (2019) 351–361

Contents lists available at ScienceDirect

Cancer Letters

journal homepage: www.elsevier.com/locate/canlet

Original Articles

Exosomes derived from human umbilical cord mesenchymal stromal cells deliver exogenous miR-145-5p to inhibit pancreatic ductal adenocarcinoma progression

Yixuan Ding[a], Feng Cao[a], Haichen Sun[a], Yecheng Wang[a], Shuang Liu[a], Yanchuan Wu[b], Qingye Cui[a], WenTong Mei[a], Fei Li[a,*]

[a] Department of General Surgery, Xuanwu Hospital, Capital Medical University, Beijing, 100053, China
[b] Department of Central Laboratory, Xuanwu Hospital, Capital Medical University, Beijing, 100053, China

ARTICLE INFO

Keywords:
PDAC
HucMSC
Exosomes
MiR-145-5p
Treatment

ABSTRACT

The roles of miRNAs in the development of cancer have made them promising tools for novel therapeutic approaches. However, the successful delivery of miRNAs to cancer cells has been hampered by difficulties in developing an effective and sustainable delivery mechanism. Exosomes are small endogenous membrane vesicles that mediate communication between cells by delivering genetic materials. Thus, given their intrinsic properties, exosomes have been a focus for use as biological delivery vehicles for miRNAs transfer. Whether exosomes can effectively deliver exogenous miRNAs to pancreatic ductal adenocarcinoma (PDAC) cells has not been thoroughly investigated. Here, we used exosomes from human umbilical cord mesenchymal stromal cells (hucMSCs) to deliver exogenous miR-145-5p, which inhibited PDAC cell proliferation and invasion and increased apoptosis and cell cycle arrest, concomitant with decreased Smad3 expression *in vitro*. Using a mouse model, we also demonstrated that overexpressing miR-145-5p significantly reduced the growth of xenograft tumors *in vivo*. Our findings provide novel insights that exosomes might be an attractive therapeutic vehicle for the clinical administration of miRNAs in patients with PDAC.

1. Introduction

Pancreatic ductal adenocarcinoma (PDAC) is the fourth most common cause of cancer-related death in the USA, and the incidence and mortality due to PDAC are closely paralleled [1]. Indeed, the overall 5-year survival rate for patients is as low as 3%–8%, which can be ascribed to approximately 52% of patients remaining asymptomatic until late in their advanced stage [2]. This dismal prognosis is a result of a lack of early effective diagnosis and resistance to systemic therapies by intrinsic characteristics [3,4]. As a consequence, there is an urgent need for clinicians and researchers to develop new optimal therapeutic strategies for PDAC patients.

The transforming growth factor-β (TGF-β) signaling pathway plays a crucial role in tumorigenesis and the progression of carcinomas [5]. Moreover, the TGF-β signaling pathway has been identified as one of ten core molecular pathways that are significantly altered in PDAC and the increased TGF-β levels in the serum or tumor tissues of PDAC patients have been correlated with poor prognosis [6,7]. This phenomenon is widely associated with the oncogenic roles of epithelial-mesenchymal transition (EMT), which has been shown to strongly correlate with local progression, distal metastasis and chemoresistance in PDAC [8]. As an intracellular direct mediator of the TGF-β signaling pathway, Smad3 plays a critical role in TGF-β-mediated EMT, resulting in tumor invasion and metastasis [9]. Furthermore, upregulation of Smad3 in PDAC patients correlated with EMT-like features, vascular invasion, lymph node metastasis, and poor prognosis, such as shorter overall survival and early recurrence [10]. However, the miRNA-based regulatory mechanism on the basis of Smad3 in TGF-β-mediated EMT of PDAC has been poorly illuminated.

The application of microRNAs (miRNAs), short single-stranded noncoding RNA molecules of 18–25 nucleotides in length that play a central role in the post transcriptional regulation of target gene expression by degrading or inhibiting the 3'-untranslated region (3'-UTR) of mRNA, may emerge as an attractive prognostic, diagnostic and

Abbreviations: PDAC, pancreatic ductal adenocarcinoma; HucMSC, human umbilical cord mesenchymal stromal cell; 145-exo, Exosomes transfected with miR-145-5p mimics; NC-exo, Exosomes transfected with negative control miRNA

* Corresponding author. Department of General Surgery, Xuanwu Hospital, Capital Medical University, 45 Changchun Street, Beijing, 100053, China.
E-mail address: lifei20180619@163.com (F. Li).

https://doi.org/10.1016/j.canlet.2018.10.039
Received 21 June 2018; Received in revised form 14 September 2018; Accepted 25 October 2018
0304-3835/ © 2018 Elsevier B.V. All rights reserved.

therapeutic tool for better treatment of PDAC [11,12]. Moreover, miR-145-5p is a tumor suppressor that is frequently downregulated in various types of cancer including hepatocellular carcinoma, gastric cancer, colorectal cancer, breast cancer, and PDAC [13–18]. It has been demonstrated that miR-145-5p participates in PDAC treatment by suppressing the expression of oncogenes, such as angiopoietin-2 and NEDD9, suggesting that miR-145-5p may be relevant in clinical therapy by inhibiting PDAC cells [19,20]. Indeed, the 3'-UTR of Smad3 is predicted to be a target of miR-145-5p, and the expression of Smad3 has been downregulated by miR-145-5p in non-small cell lung cancer and nasopharyngeal cancer, respectively [21,22]. Thus, we hypothesized that miR-145-5p could affect TGF-β-mediated EMT and tumor proliferation and invasion by regulating Smad3 in PDAC.

However, the successful delivery of miRNAs to cancer cells has been hampered by difficulties in developing an effective and sustainable delivery mechanism. Exosomes are small endogenous membrane vesicles that mediate communication between cells by carrying proteins and nucleic acids [23,24]. In fact, human mesenchymal stem cells (MSCs) are the ideal source of exosomes for drug delivery, as MSCs are readily available proliferative, immunosuppressive, and have intrinsic homing ability and a clinically tested character [25]. It has been demonstrated that human umbilical cord mesenchymal stromal cell (hucMSC) derived exosomes are safe for use in animal models and exhibit intrinsic therapeutic effects in heart and hepatic disease [26–28]. Furthermore, recent studies have revealed that exosomes can deliver tumor-suppressive miRNAs into cancer cells, thereby possibly enabling a clinically relevant exosome-based miRNA theraoeutic strategy for PDAC [29].

The current study utilized hucMSC exosomes overexpressing miR-145-5p, as a therapeutic tool to treat PDAC. Further experiments confirmed that overexpressing miR-145-5p significantly inhibited PDAC cell proliferation and invasion, which was associated with the downregulation of Smad3. Moreover, overexpressing miR-145-5p led to upregulation of epithelial markers E-cadherin, concurrent with downregulation of the mesenchymal markers N-cadherin. In addition, expression of the apoptosis-related gene Bax was increased compared with significant downregulation of Bcl-2. Furthermore, flow cytometric analysis revealed an increase in apoptotic cells among miR-145-5p-treated PDAC cells and an increase in the percentage of G0/G1 stage cells in the cell cycle. Similarly, in a mouse model of PDAC, overexpression of miR-145-5p corresponded to smaller tumor volume and weight, with downregulation of Smad3, N-cadherin, and Bcl-2 expression and upregulation of E-cadherin, and Bax expression. Our findings provide novel insights into a PDAC therapy strategy based on hucMSC exosomes.

2. Materials and methods

2.1. Isolation and identification of hucMSCs

Fresh umbilical cords were isolated from mothers at XuanWu Hospital of Capital Medical University. This experimental protocol was approved by the hospital's ethics committee, and informed consent was obtained from each patient and their relatives. The cords were rinsed three times with Dulbecco's phosphate-buffered saline (PBS) supplemented with 1% penicillin and streptomycin (Gibco, USA), and the vessels were removed. The washed cords were subsequently cut into 1 mm^3 fragments, maintained in MesenCult-ACF Basal Medium containing L-glutamine (serum-free culture medium) (Stem Cell Technologies, Canada), and incubated at 37 °C with 5% CO_2.

HucMSCs from passages 3–8 were used for all experiments. HucMSCs were cultured in hucMSCs osteogenic, or adipogenic differentiation media (Cyagen, USA) for differentiation, and differentiated cells were identified by Alizarin Red staining and Oil Red O staining, respectively. The phenotype profile of hucMSCs was evaluated through flow cytometry analysis using PE-labeled human anti-CD34, anti-CD45, anti-CD90, anti-CD73, anti-CD105, and anti-HLA-DR (all from Biolegend, USA). At least 10,000 events were acquired on a FACSCanto plus instrument (BD Bioscience), and the results were analyzed using FlowJo software (Tree Star, Ashland, OR).

2.2. Cell culture

Human pancreatic cancer cell lines Capan-1, CFPAC-1, BxPC-3, and Panc-1and normal human pancreatic duct epithelial cells (HPDEC) were purchased from Cell Bank of the Chinese Science Academy (Shanghai, China) and maintained at 37 °C in a 5% CO_2 incubator in RPMI 1640 medium (PANC-1, Capan-1 and BxPC3) or DMEM (CFPAC-1, HPDEC) with 10% fetal bovine serum (FBS) and 1% streptomycin sulphate and penicillin, respectively (all from Gibco, USA).

2.3. Isolation and purification of hucMSCs exosomes

After 3 days of incubation, the hucMSCs were cultured until ~80% confluent in culture dishes. The exosomes were isolated from the supernatants using the exosome precipitation solution, Total Exosome Isolation (Invitrogen, CA). Briefly, the cell supernatants were centrifuged at 2000 × *g* for 30 min to remove cells and debris. A volume of 0.5 Total Exosome Isolation reagent was added, and the samples were incubated at 2 °C–8 °C overnight. The samples were then centrifuged at 10,000 × *g* for 1 h at 4 °C. Finally, the pellet was resuspended at the bottom of the tube in a convenient volume of 100–1000 μl of 1 × PBS. The particle size distribution and concentration of hucMSC exosomes were measured using a ZetaView (Particle Metrix, Germany) according to the operating instructions.

2.4. Transmission electron microscopy

The purified hucMSC exosomes were fixed with 4% paraformaldehyde (Electron Microscopy Science, USA) in PBS at ambient temperature. Then, the fixed hucMSC exosomes were dropped onto a carbon-coated copper grid and fixed with 4% paraformaldehyde for 30 s. The grid was examined using a transmission electron microscope (JEM-1400plus, Japan).

2.5. Transient transfection

PDAC cells were cultured until ~50% confluence in 6-well plates, and the medium was changed to serum-free culture medium. Exosomes were loaded with miR-145-5p mimics and negative control miRNA by Exo-Fect™ Exosome Transfection Reagent (System Biosciences, USA). Briefly, 150 μl total transfection reaction containing 10 μl Exo-Fect solution, 20 pmol miRNA, 70 μl sterile 1 × PBS and 50 μl purified exosomes. The exosome transfection solution was incubated at 37 °C in a shaker for 10 min, and then, 30 μl of the ExoQuick-TC reagent was added to stop the reaction on ice for 30 min. The sample were centrifuged for 3 min at 13000–14000 rpm, and the transfected exosome pellet was resuspend in 300 μl 1 × PBS. At least 150 μl of transfected exosomes were added to approximately 1×10^5 cells per well in a 6-well culture plate.

2.6. RNA isolation and quantitative real-time PCR

Total RNA and miRNA were extracted from PDAC cells or tumor samples using an RNAprep Prue Cell/Bacteria Kit and a miRcute miRNA isolation kit (TIANGEN, Beijing, China) according to the manufacturer's protocol. Then, the RNA was reverse transcribed to cDNA using a FastKing RT Kit and miRcute Plus miRNA First-strand cDNA Synthesis Kit (TIANGEN, Beijing, China). Quantitative real-time PCR was performed using a LightCycler® 480 system (Roche Molecular Diagnostics, Pleasanton, CA, USA). All of the primers for quantitative real-time PCR were purchased from Sangon Biotech (Shanghai, China). The relative

expression of mRNAs or miRNA was evaluated by the $2^{-\Delta\Delta Ct}$ method and normalized to GAPDH or U6, respectively. Each experiment was performed three times with 3 replicates per group.

2.7. Cell proliferation assay and invasion assay

Cell proliferation assays were performed using a Cell Counting Kit-8 assay (Dojindo, Tokyo, Japan). Briefly, 3×10^3 PDAC cells were plated per well in 96-well plates and treated with exosome alone, NC-exo or 145-exo for 96 h; control cells were left untreated. Absorbance was measured at 450 nm using a 96-well plate reader (Thermo Fisher Scientific, Inc.). The cell invasion assay was analyzed using Transwell chambers coated with Matrigel (Corning, USA). Then, 4×10^4 PDAC cells from the control, exosome alone, NC-exo and 145-exo groups in 100 µl DMEM or RPMI-1640 medium without FBS were plated on the upper chamber containing the Matrigel-coated membrane matrix, and the lower chamber was filled with 500 µl DMEM or RPMI-1640 medium supplemented with 10% FBS to stimulate cell invasion. After 48 h of incubation, cells on the upper membrane surface were removed from the bottom of the filter, fixed with 4% paraformaldehyde, and stained with 5% crystal violet; 5 random fields were captured under an inverted microscope (Olympus Corporation, Tokyo, Japan) for quantification of each well.

2.8. Flow cytometry analysis of cell cycle and cell apoptosis

Cells were plated in 6-well plates at a concentration of 1×10^6/well and treated with NC-exo or 145-exo. At 48 h after treatment, cell cycle and cell apoptosis were detected using a Cell Cycle Detection Kit and an Annexin V-FITC Apoptosis Detection Kit (Nanjing KeyGen Biotech., China) according to the manufacturer's instructions. The cell cycle and percentage of apoptotic cells were evaluated using a FACSCanto plus (BD Biosciences). At least 10,000 events were acquired, and the results were analyzed using FlowJo software.

2.9. Western blotting

Cells, exosomes and tumor samples were lysed with RIPA buffer containing Phenylmethanesulfony fluoride (PMSF) (Beyotime Biotechnology, Jiangsu, China). The protein content of different fractions was detected via the BCA method. Equivalent amounts of protein (50 µg) were separated by 10% SDS-PAGE, transferred to PVDF membranes (Merck Millipore, Darmstadt, Germany), and blocked with 5% nonfat dry milk (BD Biosciences, USA) in TBST for 1 h at room temperature. The membrane was incubated with primary antibodies such as CD9, CD81, Smad3, E-cadherin, N-cadherin, Bax, Bcl-2 and GAPDH antibodies (all from Abcam) with 5% nonfat dry milk overnight at 4 °C. After incubating with the HRP-conjugated secondary antibody (Abcam, USA) at a dilution of 1:5000 with 5% nonfat dry milk for 1 h at room temperature, the bands were visualized and analyzed on an FluorChemHD2 system (ProteinSimple, USA).

2.10. Luciferase (Gluc) activity assays

The 3'-UTR of Smad3 constructs containing predicted miR-145-5p seed-matching sites from the cDNA library was amplified by PCR and, then cloned into pmiR-RB-REPORT-3'-UTR (wild type and mutant type) and 50 nM miR-145-5p mimics, 100 nM miR-145-5p inhibitor, and negative control miRNA (Ribobio, guangzhou, China) using Lipofectamine 2000 (Invitrogen, USA) according to the manufacturer's manual. After 48 h, cells were lysed with a dual luciferase assay kit (Ribobio, Guangzhou, China), and luciferase activities were calculated and normalized to the control. After treatment with recombinant human TGF-β1 (R&D Systems, USA) at 10 ng/ml for 24 h, Panc-1 cells were harvested and dual luciferase reporter assay was performed according to the manufacturer's instructions.

2.11. Mouse model study

Six-week-old male BALB/c nude mice were purchased from Capital Medical University and housed under specific pathogen-free conditions. All experimental procedures were approved by the Institutional Animal Care and Use Committee of Capital Medical University. Mice were randomly allocated into control, exosomes alone, NC-exo and 145-exo treat groups (n = 5/group). The nude mice were inoculated subcutaneously on both flanks with human pancreatic cancer Panc-1 cells (1×10^6). After 7 days of tumor growth, exosomes alone, NC-exo, and 145-exo suspension were directly administered via intra-tumor injection for three days per week. PBS was administered to the control group. On day 35, mice were killed, and tumors were removed for examination. Xenograft volumes were calculated using the formula: Volume (mm^3) = $L \times W^2/2$ (L represents length and W represents width).

2.12. Immunohistochemistry

The tumor tissue sections were incubated with an antibody to Ki-67 (Abcam, Cambridge, MA), followed by an HPR-conjugated secondary antibody. The nuclei were counterstained with Harris's hematoxylin. Cell apoptosis was assessed using a terminal TUNEL assay with an In Situ Cell Death Detection Kit (Roche, Germany) according to the manufacturer's instructions.

2.13. Clinical samples

All clinical samples were collected from the Department of General Surgery, Xuan Wu Hospital, Capital Medical University, Beijing, China, with written informed consent from all human participants. Approval for the study was granted by the Institute Research Ethics Committee at the Capital Medical University.

2.14. Statistical analysis

The statistical analyses were performed with GraphPad Prism 7.0. Each experiment was repeated at least thrice, and the data are expressed as the mean ± SD. Statistical significance was determined using Student's *t*-test or one-way analysis of variance. Correlation studies were performed to show the expression of miR-145-5p and Smad3. A P value of 0.05 or less was considered statistically significant.

2.15. Data availability

The data that support the findings of this study are available in the article. The microarray data and Smad3 expression data have been deposited in The Cancer Genome Atlas (TCGA). Smad3 expression data have been deposited in the Oncomine database under accession code Badea Pancreas and Collisson Pancreas.

3. Results

3.1. MiR-l45-5p and Smad3 expression of PDAC in vitro and in vivo

To identify whether miR-145-5p is involved in the regulation of PDAC progression, the expression of miR-145-5p and Smad3 was analyzed by quantitative real-time PCR. MiR-145-5p expression was significantly decreased in four PDAC cell lines, corresponding to a significant upregulation of Smad3 expression, compared with normal pancreatic duct epithelial cells (Fig. 1A and B). Similarly, miR-145-5p expression was significant downregulated in eight primary PDAC tissues, concurrent with a significant increase in Smad3 expression relative to adjacent normal pancreatic tissues (Fig. 1C and D). Moreover, the expression levels of miR-145-5p and Smad3 were analyzed in eight freshly enrolled PDAC tissues, and the correlation studies showed that

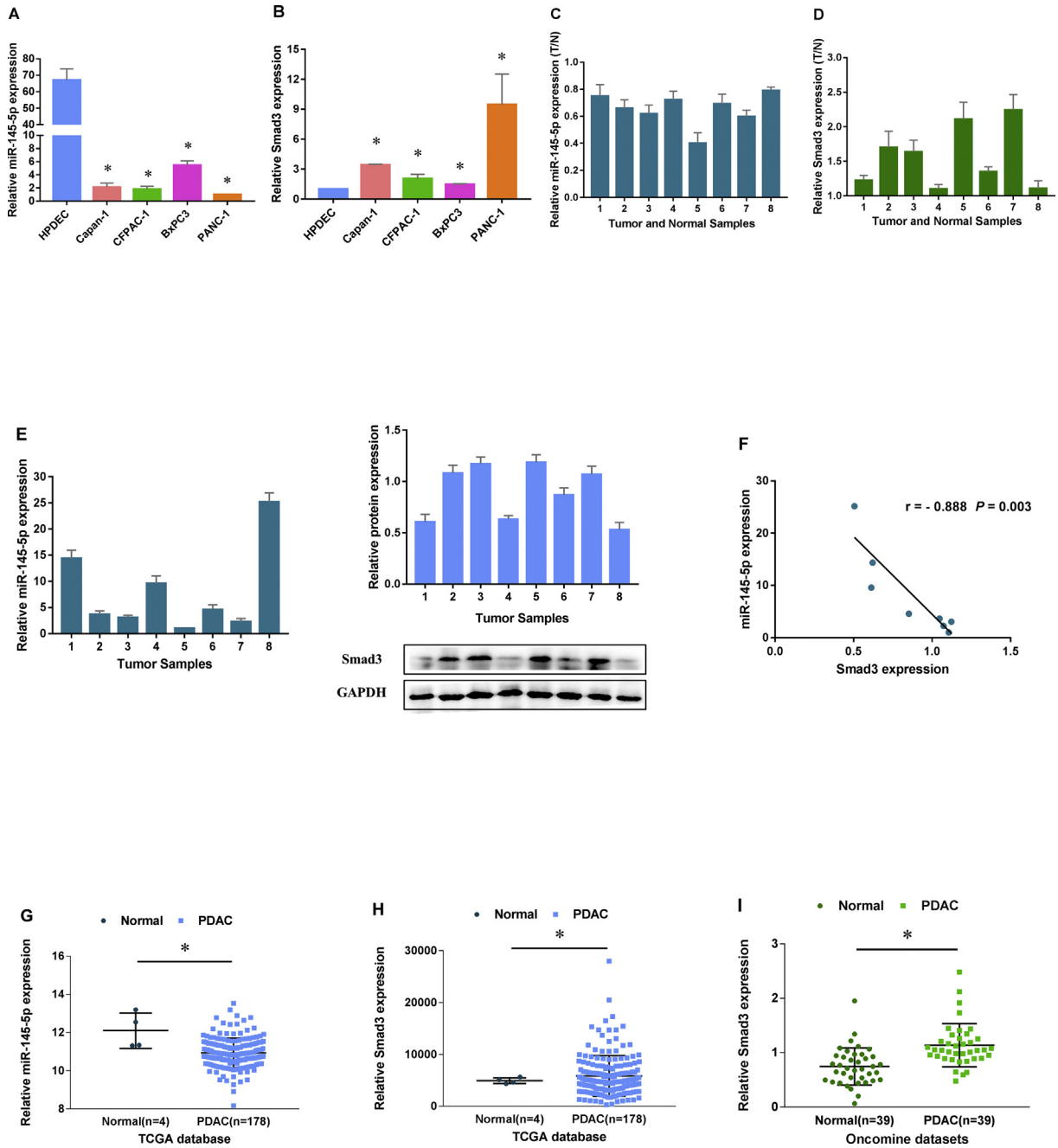

Fig. 1. MiR-l45-5p and Smad3 expression of PDAC *in vitro* and *in vivo*. (A–B) Four PDAC cell lines displayed downregulated expression of miR-145-5p, corresponding to upregulated expression of Smad3, compared with normal human pancreatic duct epithelial cells. (C–D) The eight primary PDAC tissues (T) showed downregulated expression of miR-145-5p, concurrent with upregulated expression of Smad3, compared with normal pancreatic tissues (N). (E) The expression profiles of miR-145-5p and the expression levels of Smad3 protein in eight freshly collected human PDAC tissue samples. The expression of miR-145-5p was examined using quantitative real-time PCR analysis and normalized by U6 expression. Sample T5 was used as a standard, and the fold change in miR-145-5p expression in other samples was calculated by comparing with the miR-145-5p/U6 ratio in sample T5. The expression levels of Smad3 were examined using Western blotting. GAPDH was used as a loading control. Data are representative of three independent experiments and presented as the mean ± SD of the mean. $^{*}P < 0.05$, $^{**}P < 0.01$. (F) Correlation between miR-145-5p expression and Smad3 expression in the PDAC tissue samples. (G–H) MiR-145-5p expression was decreased and Smad3 expression was increased in PDAC tissues (n = 178) compared with normal tissues (n = 4) based on the TCGA database. (I) Smad3 expression was overexpressed in PDAC tissues (n = 39) compared with normal tissues (n = 39) based on the Oncomine datasets. Data are representative of three independent experiments and presented as the mean ± SD of the mean. $^{*}P < 0.05$.

miR-145-5p levels were inversely correlated with Smad3 (r = - 0.888; $P = 0.003$) protein levels (Fig. 1E and F). Additionally, the TCGA database showed that miR-145-5p expression was decreased and Smad3 expression was increased in PDAC tissues relative to normal pancreatic tissues (Fig. 1G and H). The Oncomine datasets showed that Smad3 expression was overexpressed in PDAC tissues relative to the normal pancreatic tissues (Fig. 1I). Collectively, these results indicated a downregulation of miR-145-5p and upregulation of Smad3 expression in PDAC *in vitro* and *in vivo*.

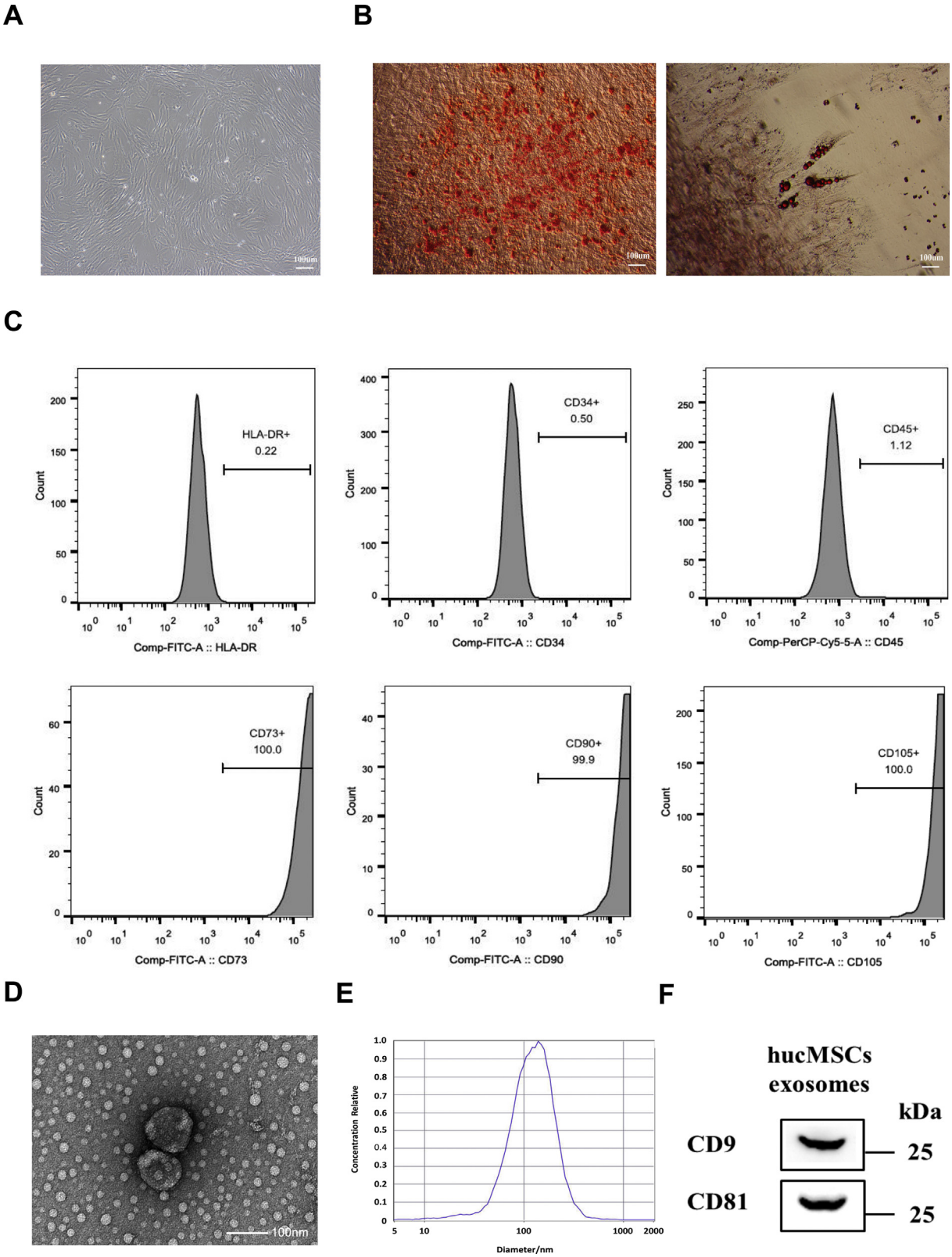

Fig. 2. Isolation and characterization of exosomes derived from hucMSCs. (A) The cell morphology of hucMSCs (passage 3) was observed under a light microscope (magnification, × 100). (B) Representative images of osteocytes (× 100) and adipocytes (× 100) differentiation of hucMSC cultured in the differentiation media. The cells were analyzed using cytochemical staining with Alizarin Red and Oil red O, respectively. (C) Flow cytometry analysis of the surface markers of hucMSC. (D) Transmission electron microscopic images of hucMSC exosomes. The scale bars indicate 100 nm. (E) The size distribution of the hucMSC exosomes was examined using a ZetaView. (F) The positive expression of markers CD9 and CD81 in hucMSC exosomes was detected by Western blotting.

3.2. Isolation and characterization of exosomes derived from hucMSCs

The hucMSCs were purified and confirmed on the basis of the criteria defined by the International Society for Cellular Therapy [30]. The cell morphology of hucMSCs (passage 3) was observed under a light microscope (magnification, × 100) (Fig. 2A). Positive cytochemical staining for Alizarin Red and Oil Red was observed after osteogenic and adipogenic induction of hucMSCs, respectively. (Fig. 2B). Moreover, hucMSCs positively expressed CD73, CD90, and CD105 but negatively expressed CD34, CD45, and HLA-DR. (Fig. 2C). Exosomes were isolated and purified from the hucMSC-conditioned medium. HucMSC exosomes had a characteristic 'saucer-like' morphology with diameters that ranged from 52.5 nm to 185.5 nm, with an average of 119 nm and the concentration of hucMSC exosomes was 4.0×2^{10} Particles/mL (Fig. 2D and E). Further results showed positive expression of exosomal markers, such as CD9 and CD81 (Fig. 2F).

3.3. Exosomes engineered to express miR-145-5p

Exosomes loaded with miR-145-5p mimics (145-exo) and negative control miRNA (NC-exo) were added to PDAC cells. To assess the endocytosis efficiency of miR-145-5p produced by exosomes, Panc-1 cells with 145-exo were detected by qPCR assay. There was a significant increase in miR-145-5p expression in Panc-1 cells treated with 145-exo, compared with NC-exo (Fig. 3A), confirming that miR-145-5p expression in Panc-1 cells was increased and endocytosed via hucMSC exosomes. To visualize the process of miR-145-5p delivery from exosomes to Panc-1 cells, Texas Red-labeled siRNA was transfected into exosomes as a positive control. After 24 h of culture, Texas Red-labeled siRNA was evident in the cytoplasm of Panc-1 cells followed by intracellular visualization using immunofluorescence microscopy (Fig. 3B). Thus, these data confirmed that hucMSC-derived exosomes can effectively deliver miR-145-5p into Panc-1 cells *in vitro*.

3.4. MiR-145-5p overexpression inhibits proliferation and invasion of PDAC cells

The biological function of miR-145-5p in the progression of PDAC was investigated by adding 145-exo into Capan-1, CFPAC-1, BxPC3 and Panc-1 PDAC cell lines. CCK-8 assays demonstrated that miR-145-5p overexpression inhibits proliferation of PDAC cells (Fig. 4A). Transwell assays demonstrated that overexpression of miR-145-5p significantly decreased the invasiveness capability of PDAC cells (Fig. 4B). Flow cytometric analysis revealed that miR-145-5p caused an increase in the percentage of the cells in the G0/G1 stage of the cell cycle from 32.82 ± 1.2% (NC-exo) to 43.45 ± 1.3% (145-exo) (Fig. 4C). Subsequently, we observed an increase in apoptotic cells among 145-exo-treated PDAC cells, relative to NC-exo treated cells (Fig. 4D). These data indicated that 145-exo can inhibit the proliferation of PDAC cells by enhancing cell apoptosis and cell cycle arrest.

3.5. Suppressor miR-145-5p directly targets Smad3 in PDAC cells by exosomes

We first searched miRNA databases for potential miR-145-5p target genes that may contribute to or promote PDAC progression. Three public miRNA databases (miRBase, TargetScan and MicroRNA) all predicted that Smad3 might be a potential target for miR-145-5p (Fig. 5A), which has been reported by previous publication [31]. The 3'-UTR of Smad3 contains a highly conserved binding site from position 1397 to 1404 or from position 3922 to 3929 in different species (Fig. 5B). The results showed that Smad3 protein expression was significantly downregulated in PDAC cells upon addition of 145-exo. We also found that 145-exo led to upregulation of the epithelial markers E-cadherin, concurrent with downregulation of the mesenchymal markers N-cadherin. Moreover, the expression of the apoptosis-related gene Bax was increased compared with a significant downregulation of Bcl-2 (Fig. 5C). We performed a luciferase reporter assay by cotransfecting a vector containing the wild-type (WT) or mutant (MUT) Smad3 3'UTR-fused luciferase together with miR-145-5p mimics or negative control miRNA. Overexpression of miR-145-5p decreased the luciferase activity of the wild type in Panc-1 cells. However, the mutant Smad3 3'UTR entirely restored luciferase activity (Fig. 5D). Moreover, the TGF-β-induced luciferase activity was significantly suppressed in Panc-1 cells by overexpression of miR-145-5p; whereas silencing of miR-145-5p increased luciferase activity in these cells (Fig. 5E). Collectively, these results demonstrated that miR-145-5p is directly associated with the mRNA 3'UTR regions of Smad3.

3.6. MiR-145-5p overexpression inhibits proliferation of PDAC cells in vivo

To investigate whether 145-exo could inhibit PDAC cells *in vivo*, 145-exo was administered by intra-tumor injection to nude mice bearing human pancreatic cancer Panc-1 cells. Mice injected subcutaneously with control, exosomes alone or NC-exo showed remarkable tumor growth over 35 days. However, mice injected with 145-exo at 7 days after subcutaneous inoculation had a much smaller tumor volume and weight (Fig. 6A–D). We performed a Western blot analysis of the relative expression of Smad3, E-cadherin, N-cadherin, Bax and Bcl-2 following 35 days in the mice. There was a significant downregulation of Smad3 in 145-exo-treated tumors compared with NC-exo-treated tumors. Similarly, E-cadherin and Bax were significantly increased in 145-exo-treated tumors, concurrent with a significant decrease in N-cadherin and Bcl-2 (Fig. 6E). In addition, fewer Ki-67-positive and more TUNEL-positive cells were observed in the tumor sections from the 145-exo group than NC-exo group (Fig. 6F and G). Collectively, these data suggested that 145-exo effectively inhibits the proliferation of PDAC cells *in vivo*.

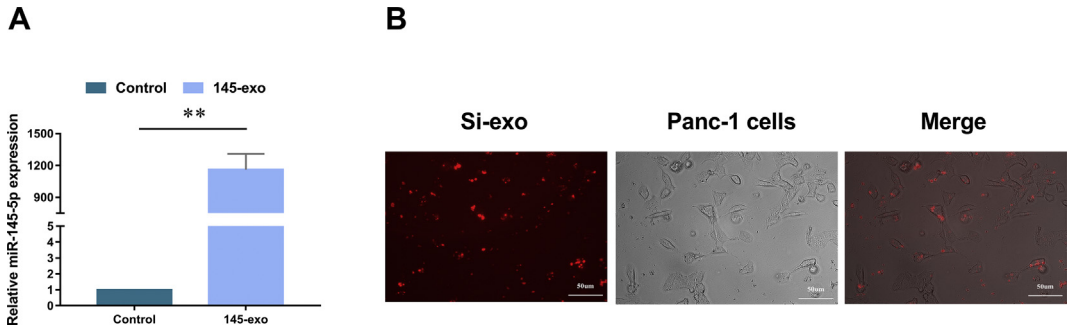

Fig. 3. Exosomes engineered to express miR-145-5p. (A) Panc-1 cells transfected with 145-exo showed a significantly increased expression of miR-145-5p in comparison with Panc-1 cells added with NC-exo. (B) Fluorescence microscopy showed that Texas Red-labeled siRNA was apparent in the cytoplasm of Panc-1 cells after 24 h. Data are representative of three independent experiments and presented as the mean ± SD of the mean. $^{*}P < 0.05$, $^{**}P < 0.01$.

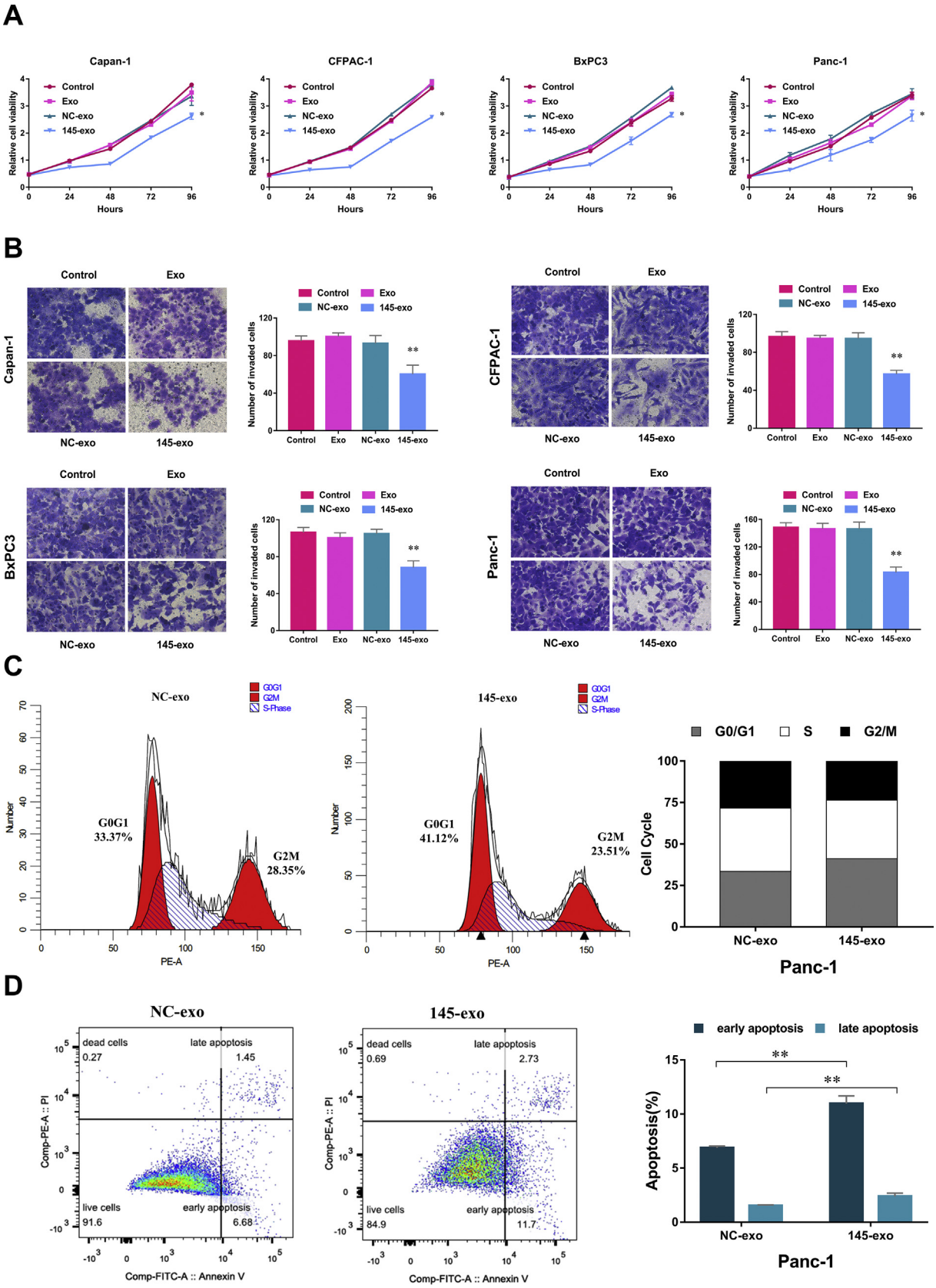

Fig. 4. MiR-145-5p overexpression inhibits proliferation and invasion of PDAC cells. (A) Proliferation of PDAC cells treated as indicated. Cell viability was detected from 0 to 96 h after transfection using the CCK-8 array. (B) The invasive properties of PDAC cells after transfection using a Matrigel-coated Boyden chamber. Magnification, × 400. (C) Cell cycle analysis revealed an increase in the G0/G1 population among 145-exo-treated Panc-1 cells. (D) Apoptotic cells were determined by staining with Annexin V -FITC and propidium iodide (PI) after the treatment. Data are representative of three independent experiments and presented as the mean ± SD of the mean. $^{*}P < 0.05$, $^{**}P < 0.01$.

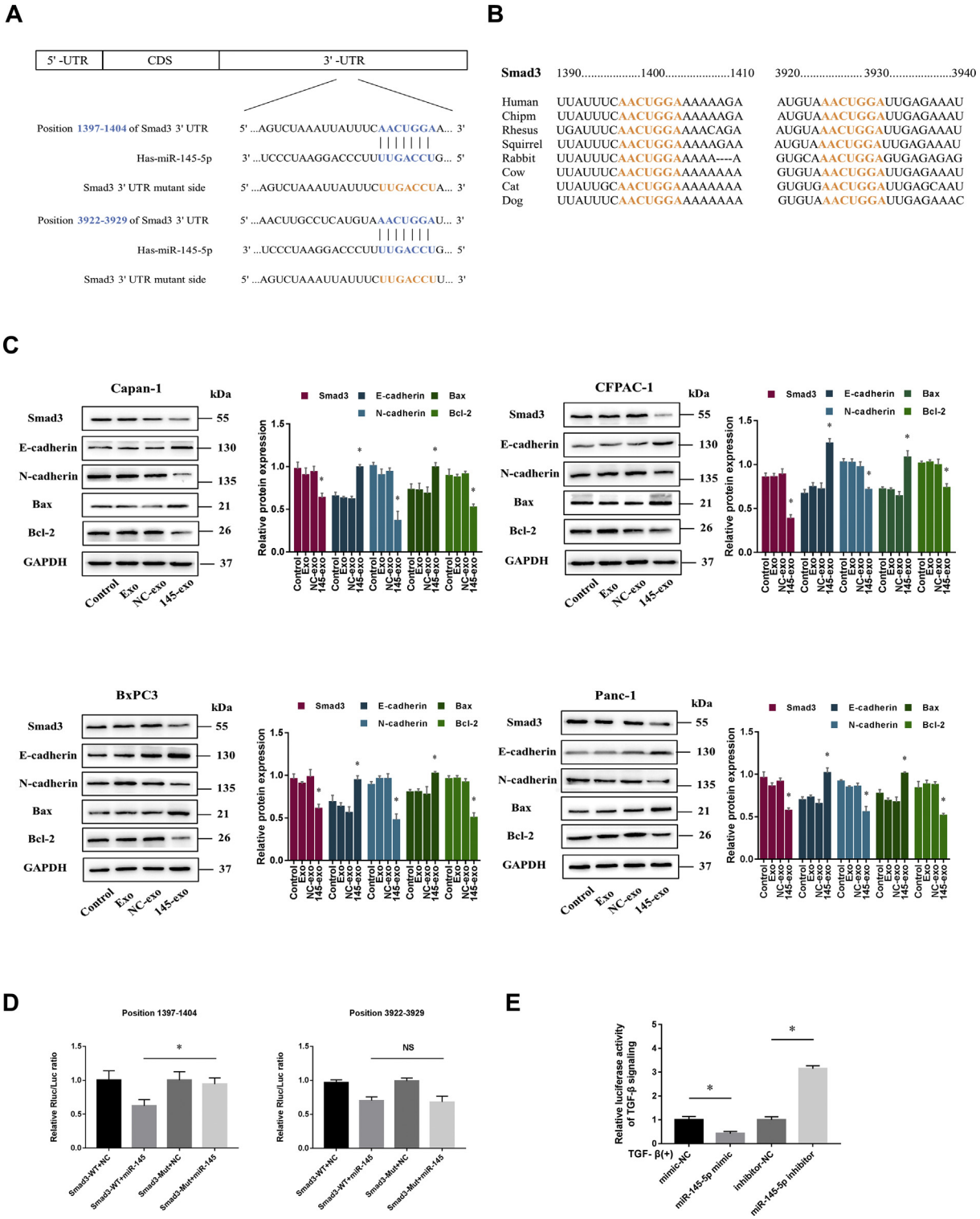

Fig. 5. Suppressor miR-145-5p directly targets Smad3 in PDAC cells by exosomes. (A) Schematic diagram of the putative binding sites of miR-145-5p in the wild-type Smad3 3'UTR (in blue). The miR-145-5p seed sequence matches in the Smad3 3'UTR are mutated at the positions as indicated (in orange). (B) Potential miR-145-5p binding sites on Smad3 (in orange) are broadly conserved among different species. (C) Expression of the target genes Smad3, the epithelial markers E-cadherin, the mesenchymal markers N-cadherin, and apoptosis-related genes Bax and Bcl-2 in PDAC cells assessed by Western blot, following transfection with exosomes alone, NC-exo or 145-exo for 48 h. GAPDH was used as a loading control. (D) Luciferase activity assays of WT and MUT Smad3 3'UTR luciferase reporters after cotransfection with miR-145-5p mimic and negative control miRNA in Panc-1 cells. The normalized luciferase activity of transfected control mimic miRNA was set as a relative luciferase activity of 1. (E) Luciferase assay showed suppression of TGF-β-induced p3TP-lux transcriptional activity by miR-145-5p in Panc-1 cells. Data are representative of three independent experiments and presented as the mean ± SD of the mean. $^*P < 0.05$.

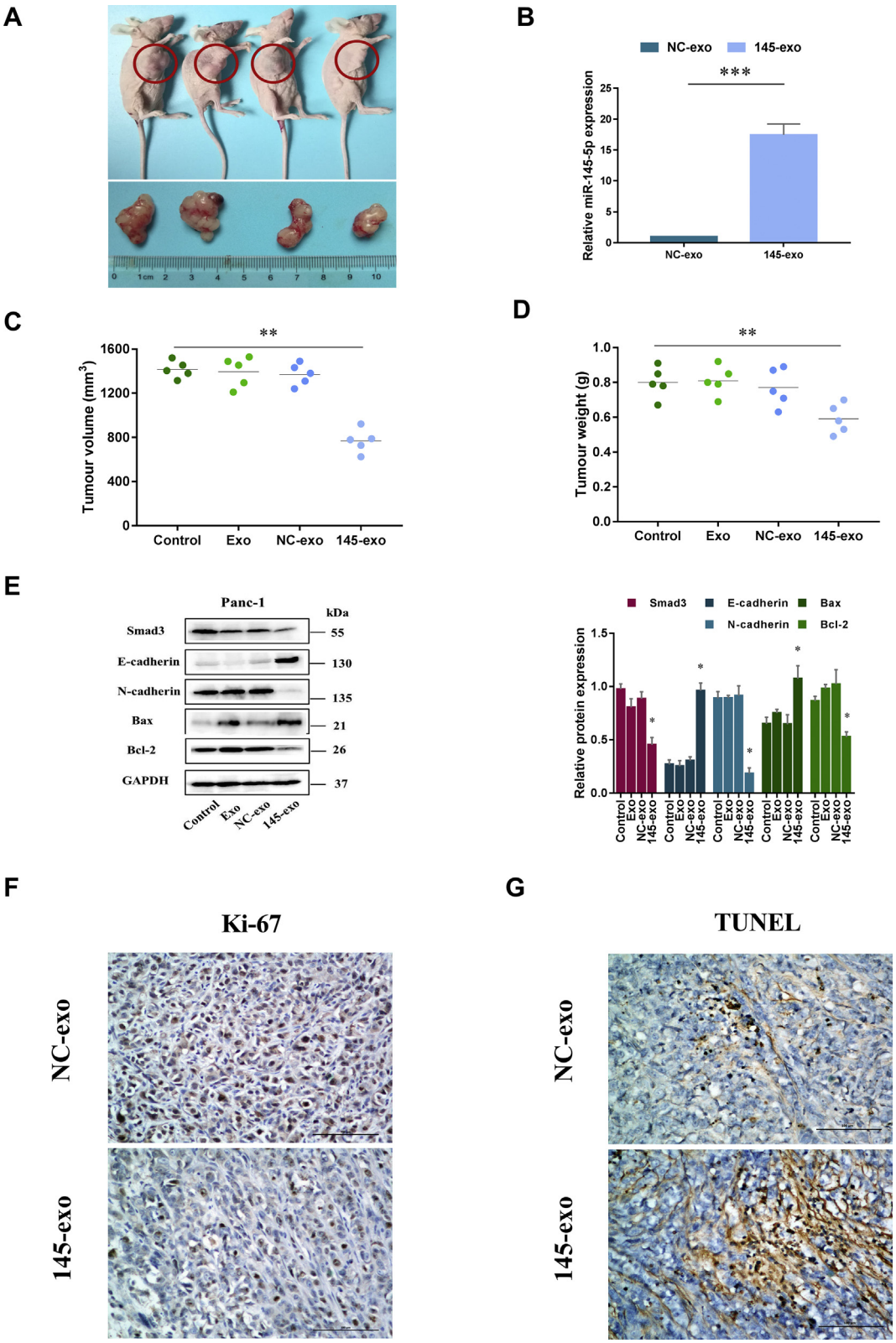

Fig. 6. MiR-145-5p overexpression inhibits proliferation of PDAC cells *in vivo*. (A) Representative images of xenografts in Panc-1 tumor-bearing nude mice (n = 5 mice per group) at 35 days postimplantation (28 days after 145-exo administration). (B) Changes of miR-145-5p expression in 145-exo compared to NC-exo. (C–D) Changes in tumor volumes and weight in the Panc-1 xenograft model at 35 days postimplantation. (E) Western blot analysis showing the levels of Smad3, E-cadherin, N-cadherin, Bcl-2 and Bax in the tumor samples. GAPDH was used as a loading control. (F–G) Ki-67 and TUNEL immunohistochemical staining on tumor sections from the NC-exo and 145-exo group. The images are shown at × 200. Data are representative of three independent experiments and presented as the mean ± SD of the mean. $^{*}P < 0.05$, $^{**}P < 0.01$.

4. Discussion

The contribution of miRNAs to the pathogenesis and progression of PDAC suggests that their utility can be exploited for the development of novel therapeutic strategies. However, the application of miRNA therapies has been hampered in that viruses and liposomes deliver miRNA to cancer cells in an unsafe and low-efficiency manner [32]. Exosomes are endogenous nanoparticles that can serve as a novel drug delivery mechanism that combines non-immunogenicity, specificity targeting ability, and a high drug carrying capacity, making them useful in tumor therapy [33]. Thus, the use of exosomes as biological vehicles to delivery exogenous tumor suppressor miRNAs or chemotherapy drugs is a promising approach. In addition, MSCs are an efficient mass producer of exosomes for drug delivery, and secreted exosomes have been tested in numerous clinical trials [34]. The novel mechanism of intercellular communication mediated via exosomes has been demonstrated by exosome-mediated transfer of miR-122 to hepatocellular carcinoma cells (HCC). In this study, adipose-derived mesenchymal stem cells (AMSCs) could effectively package miR-122 into secreted exosomes, which can increase the sensitivity of chemotherapeutic agent sorafenib by reducing target gene expression in HCC cells [35]. Our data indicated a potential and feasible therapeutic strategy that uses hucMSC exosomes as an effective and specific vehicle to deliver exogenous miR-145-5p to PDAC cells.

The present study reported that hucMSC exosomes, successfully engineered to overexpress miR-145-5p, are able to deliver miR-145-5p through endocytosis in both *in vitro* and *in vivo* models of PDAC. As a result, 145-exo can effectively inhibit the proliferation and invasion of PDAC cells and can enhance PDAC cell apoptosis and cell cycle arrest. Regarding the target gene of miR-145-5p, Smad3 is involved in the promotion of PDAC progression through EMT induction and acts as a promising biomarker of poor prognosis of PDAC [10]. *In vitro* experiments indicated that 145-exo treatment resulted in the downregulation of Smad3 expression in PDAC cells. We also found that 145-exo led to upregulation of the epithelial markers E-cadherin, concurrent with downregulation of the mesenchymal markers N-cadherin. Moreover, the expression of apoptosis-related gene Bax was increased compared with a significant downregulation of Bcl-2. Flow cytometric analysis revealed an increase in apoptotic cells among 145-exo-treated PDAC cells and cell cycle assessment suggested that 145-exo caused an increase in the percentage of cells in the G0/G1 stage of the cell cycle from 32.82 ± 1.2% (NC-exo) to 43.45 ± 1.3% (145-Exo).

An experimental BALB/c nude mice model of Panc-1 cells was used to demonstrate that hucMSC exosomes transferred exogenous miR-145-5p to the xenograft tumor by intra-tumor injection. Treated mice exhibited in a much smaller tumor volume and weight, together with downregulation of Smad3, N-cadherin and Bax expression and significant upregulation of E-cadherin and Bcl-2 expression, compared with untreated mices. However, treatment with exosomes alone cannot significantly influence tumor volume and weight. This phenomenon may be attributed to the possibility that the quantity of injected exosomes was insufficient for tumor growth inhibition, or that hucMSC exosomes may be have a role in promoting tumor growth. In fact, the function of MSCs in tumor therapy remains controversial. Several studies have shown that administered MSCs can either promote tumor development or inhibit tumor growth, both *in vitro* and *in vivo* [36,37]. This discrepancy in the effect of MSC-derived exosomes on tumor growth according to previous studies may be ascribed to tumor characteristics, MSC sources, and routes of exosome administration. A previous study reported that different sources of MSC exosomes have differential effects on glioblastoma cells [38]. Exosomes derived from bone marrow and umbilical cord MSCs decreased glioblastoma cell proliferation, while an opposite effect was observed with exosomes derived from adipose tissue MSCs.

The primary administrations routes of exosomes currently include intravenous injection, intratumoral injection, oral administration, and intraperitoneal injection. It is speculated that due to the unique lipid and protein composition of exosomes, they are more immunocompatible and have a low clearance rate. However, a previous study indicated that intravenously injected exosomes are also rapidly cleared by the liver and spleen and exhibit minimal tumor accumulation, compared with liposomes. Furthermore, when delivered intratumorally, exosomes resided longer in tumor tissues than liposomes [39]. Thus, the current study directly delivered hucMSC exosomes into the subcutaneous xenograft tumor via intratumoral injection. This rapid clearance together with minimal intratumoral accumulation of unmodified exosomes limits their use as an effective drug delivery vehicle by intravenous injection. Hence, efficient targeted drug delivery vehicles with tissue-specific, low immunogenic and nontoxic properties are needed for clinical cancer therapy. Others have demonstrated that exosomes express an exosomal membrane protein Lamp2b fused to αv integrin-specific iRGD peptide and showed highly efficient targeting and doxorubicin (Dox) delivery to αv integrin-positive breast cancer cells by intravenous injection [40]. Thus, these results suggest that exosomes modified by targeting ligands can be effectively used for the delivery of chemotherapy drugs to tumors by intravenous injection.

To our knowledge, this study provides the first evidence that engineered hucMSC exosomes delivering miR-145-5p effectively inhibit PDAC progression by regulating Smad3 expression, suggesting that exosomes can serve as novel and high-efficiency drug delivery vehicles and that miR-145-5p/Smad3 may be an important regulatory mechanism in the progression of PDAC. Our findings may offer potentially novel therapeutic strategies for the treatment of patients with PDAC. In the long term, this innovative therapeutic approach could be applied to other diseases or to clinical patients.

Conflicts of interest

The authors declare no conflict of interest.

Acknowledgements

This work was supported by the National Natural Science Foundation, China (Grant No. 81272756), and Beijing Natural Science Foundation, China (Grant No. 7162076).

References

[1] T. Kamisawa, L.D. Wood, T. Itoi, K. Takaori, Pancreatic cancer, Lancet 388 (2016) 73–85.
[2] R.L. Siegel, K.D. Miller, A. Jemal, Cancer statistics, 2017, Ca - Cancer J. Clin. 67 (2017) 7–30.
[3] A. Makohon-Moore, C.A. Iacobuzio-Donahue, Pancreatic cancer biology and genetics from an evolutionary perspective, Nat. Rev. Canc. 16 (2016) 553–565.
[4] I. Garrido-Laguna, M. Hidalgo, Pancreatic cancer: from state-of-the-art treatments to promising novel therapies, Nat. Rev. Clin. Oncol. 12 (2015) 319–334.
[5] J. Massagué, TGFβ in cancer, Cell 134 (2008) 215–230.
[6] P. Bailey, D.K. Chang, K. Nones, A.L. Johns, A.M. Patch, M.C. Gingras, et al., Genomic analyses identify molecular subtypes of pancreatic cancer, Nature 531 (2016) 47–52.
[7] A. Hilbig, H. Oettle, Transforming growth factor beta in pancreatic cancer, Curr. Pharm. Biotechnol. 12 (2011) 2158–2164.
[8] M. Beuran, I. Negoi, S. Paun, A.D. Ion, C. Bleotu, R.I. Negoi, S. Hostiuc, The epithelial to mesenchymal transition in pancreatic cancer: a systematic review, Pancreatology 15 (2015) 217–225.
[9] A.B. Roberts, F. Tian, S.D. Byfield, C. Stuelten, A. Ooshima, S. Saika, K.C. Flanders, Smad3 is key to TGF-beta-mediated epithelial-to-mesenchymal transition, fibrosis, tumor suppression and metastasis, Cytokine Growth Factor Rev. 17 (2006) 19–27.
[10] K. Yamazaki, Y. Masugi, K. Effendi, H. Tsujikawa, N. Hiraoka, M. Kitago, M. Shinoda, O. Itano, M. Tanabe, Y. Kitagawa, M. Sakamoto, Upregulated SMAD3 promotes epithelial-mesenchymal transition and predicts poor prognosis in pancreatic ductal adenocarcinoma, Lab. Invest. 94 (2014) 683–691.
[11] R. Rupaimoole, F.J. Slack, MicroRNA therapeutics: towards a new era for the management of cancer and other diseases, Nat. Rev. Drug Discov. 16 (2017) 203–222.
[12] D. Chitkara, A. Mittal, R.I. Mahato, MiRNAs in pancreatic cancer: therapeutic potential, delivery challenges and strategies, Adv. Drug Deliv. Rev. 81 (2015) 34–52.
[13] X.W. Yang, L.J. Zhang, X.H. Huang, L.Z. Chen, Q. Su, W.T. Zeng, W. Li, Q. Wang, MiR-145 suppresses cell invasion in hepatocellular carcinoma cells: miR-145 targets

ADAM17, Hepatol. Res. 44 (2014) 551–559.
[14] T. Qiu, X. Zhou, J. Wang, Y. Du, J. Xu, Z. Huang, W. Zhu, Y. Shu, P. Liu, MiR-145, miR-133a and miR-133b inhibit proliferation, migration, invasion and cell cycle progression via targeting transcription factor Sp1 in gastric cancer, FEBS Lett. 588 (2014) 1168–1177.
[15] S. Li, X. Wu, Y. Xu, S. Wu, Z. Li, R. Chen, N. Huang, Z. Zhu, X. Xu, MiR-145 suppresses colorectal cancer cell migration and invasion by targeting an ETS-related gene, Oncol. Rep. 36 (2016) 1917–1926.
[16] X. Yan, X. Chen, H. Liang, T. Deng, W. Chen, S. Zhang, et al., MiR-143 and miR-145 synergistically regulate ERBB3 to suppress cell proliferation and invasion in breast cancer, Mol. Canc. 24 (2014) 13 220.
[17] I.G. Papaconstantinou, A. Manta, M. Gazouli, A. Lyberopoulou, P.M. Lykoudis, G. Polymeneas, D. Voros, Expression of microRNAs in patients with pancreatic cancer and its prognostic significance, Pancreas 42 (2013) 67–71.
[18] J. Namkung, W. Kwon, Y. Choi, S.G. Yi, S. Han, M.J. Kang, S.W. Kim, T. Park, J.Y. Jang, Molecular subtypes of pancreatic cancer based on miRNA expression profiles have independent prognostic value, J. Gastroenterol. Hepatol. 31 (2016) 1160–1167.
[19] H. Wang, C. Hang, X.L. Ou, J.S. Nie, Y.T. Ding, S.G. Xue, H. Gao, J.X. Zhu, MiR-145 functions as a tumor suppressor via regulating angiopoietin-2 in pancreatic cancer cells, Cancer Cell Int. 16 (2016) 65.
[20] T. Han, X.P. Yi, B. Liu, M.J. MJ, Y.X. L, MicroRNA-145 suppresses cell proliferation, invasion and migration in pancreatic cancer cells by targeting NEDD9, Mol. Med. Rep. 11 (2015) 4115–4120.
[21] H. Hu, Z. Xu, C. Li, C. Xu, Z. Lei, H.T. Zhang, J. Zhao, MiR-145 and miR-203 represses TGF-β-induced epithelial-mesenchymal transition and invasion by inhibiting SMAD3 in non-small cell lung cancer cells, Lung Canc. 97 (2016) 87–94.
[22] H. Huang, P. Sun, Z. Lei, M. Li, Y. Wang, H.T. Zhang, J. Liu, MiR-145 inhibits invasion and metastasis by directly targeting Smad3 in nasopharyngeal cancer, Tumour Biol. 36 (2015) 4123–4131.
[23] H. Valadi, K. Ekström, A. Bossios, M. Sjöstrand, J.J. Lee, J.O. Lötvall, Exosome-mediated transfer of mRNAs and microRNAs is a novel mechanism of genetic exchange between cells, Nat. Cell Biol. 9 (2007) 654–659.
[24] A. Tan, J. Rajadas, A.M. Seifalian, Exosomes as nano-theranostic delivery platforms for gene therapy, Adv. Drug Deliv. Rev. 65 (2013) 357–367.
[25] R.W. Yeo, R.C. Lai, B. Zhang, S.S. Tan, Y. Yin, B.J. Teh, S.K. Lim, Mesenchymal stem cell: an efficient mass producer of exosomes for drug delivery, Adv. Drug Deliv. Rev. 65 (2013) 336–341.
[26] L. Sun, R. Xu, X. Sun, Y. Duan, Y. Han, Y. Zhao, H. Qian, W. Zhu, W. Xu, Safety evaluation of exosomes derived from human umbilical cord mesenchymal stromal cell, Cytotherapy 18 (2016) 413–422.
[27] Y. Zhao, X. Sun, W. Cao, J. Ma, L. Sun, H. Qian, W. Zhu, W. Xu, Exosomes derived from human umbilical cord mesenchymal stem cells relieve acute myocardial ischemic injury, Stem Cell. Int. 2015 (2015) 761643.
[28] T. Li, Y. Yan, B. Wang, H. Qian, X. Zhang, L. Shen, M. Wang, Y. Zhou, W. Zhu, W. Li, W. Xu, Exosomes derived from human umbilical cord mesenchymal stem cells alleviate liver fibrosis, Stem Cell. Dev. 22 (2013) 845–854.
[29] N. Kosaka, F. Takeshita, Y. Yoshioka, K. Hagiwara, T. Katsuda, M. On, T. Ochiya, Exosomal tumor-suppressive microRNAs as novel cancer therapy "Exocure" is another choice for cancer treatment, Adv. Drug Deliv. Rev. 65 (2013) 376–382.
[30] M. Dominici, K. Le Blanc, I. Mueller, I. Slaper-Cortenbach, F. Marini, D. Krause, R. Deans, A. Keating, Dj Prockop, E. Horwitz, Minimal criteria for defining multipotent mesenchymal stromal cells, Int. Soc. Cell. Ther. Position Statement, Cytotherapy 8 (2006) 315–317.
[31] H.Y. Zhu, C. L, Z. Zheng, Q. Zhou, H. Guan, L.L. Su, J.T. Han, X.X. Zhu, S.Y. Wang, J. Li, D.H. Hu, Peroxisome proliferator-activated receptor-γ (PPAR-γ) agonist inhibits collagen synthesis in human hypertrophic scar fibroblasts by targeting Smad3 via miR-145, Biochem. Biophys. Res. Commun. 459 (2015) 49–53.
[32] R. Van der Meel, M.H. Fens, P. Vader, W.W. van Solinge, O. Eniola-Adefeso, R.M. Schiffelers, Extracellular vesicles as drug delivery systems: lessons from the liposome field, J. Contr. Release 195 (2014) 72–85.
[33] D. Sun, X. Zhuang, S. Zhang, Z.B. Deng, W. Grizzle, D. Miller, H.G. Zhang, Exosomes are endogenous nanoparticles that can deliver biological information between cells, Adv. Drug Deliv. Rev. 65 (2013) 342–347.
[34] R.C. Lai, R.W. Yeo, K.H. Tan, S.K. Lim, Exosomes for drug delivery-a novel application for the mesenchymal stem cell, Biotechnol. Adv. 31 (2013) 543–551.
[35] G. Lou, X. Song, F. Yang, S. Wu, J. Wang, Z. Chen, Y. Liu, Exosomes derived from miR-122-modified adipose tissue-derived MSCs increase chemosensitivity of hepatocellular carcinoma, J. Hematol. Oncol. 8 (2015) 122.
[36] W. Zhu, L. Huang, Y. Li, X. Zhang, J. Gu, Y. Yan, X. Xu, M. Wang, H. Qian, W. Xu, Exosomes derived from human bone marrow mesenchymal stem cells promote tumor growth in vivo, Cancer Lett. 315 (2012) 28–37.
[37] S. Bruno, F. Collino, M.C. Deregibus, C. Grange, C. Tetta, G. Camussi, Microvesicles derived from human bone marrow mesenchymal stem cells inhibit tumor growth, Stem Cell. Dev. 22 (2013) 758–771.
[38] A. Del Fattore, R. Luciano, R. Saracino, G. Battafarano, C. Rizzo, L. Pascucci, G. Alessandri, A. Pessina, A. Perrotta, A. Fierabracci, M. Muraca, Differential effects of extracellular vesicles secreted by mesenchymal stem cells from different sources on glioblastoma cells, Expet Opin. Biol. Ther. 15 (2015) 495–504.
[39] T. Smyth, M. Kullber, N. Malik, P. Smith-Jones, M.W. Graner, T.J. Anchordoquy, Biodistribution and delivery efficiency of unmodified tumor-derived exosomes, J. Contr. Release 199 (2015) 145–155.
[40] Y. Tian, S. Li, J. Song, T. Ji, M. Zhu, G.J. Anderson, J. Wei, G. Nie, A doxorubicin delivery platform using engineered natural membrane vesicle exosomes for targeted tumor therapy, Biomaterials 35 (2014) 2383–2390.